First-principles study of ZrO_2/Si interfaces: Energetics and band offsets

Y. F. Dong and Y. P. Feng*
Department of Physics, National University of Singapore, 2 Science Drive 3, Singapore 117542

S. J. Wang
Institute of Materials Research and Engineering, 3 Research Link, Singapore 117602

A. C. H. Huan
Department of Physics, National University of Singapore, 2 Science Drive 3, Singapore 117542
and Institute of Materials Research and Engineering, 3 Research Link, Singapore 117602
(Received 5 October 2004; revised manuscript received 31 January 2005; published 14 July 2005)

First-principles calculations for ZrO_2/Si interfaces are presented. Various model interfaces satisfying the general bonding rules were considered. The interface formation energies were evaluated as a function of oxygen potential, which shows the possibility of atomic control of the interface structure by altering the chemical environment. The strain mode and interface structure effects on band offset were investigated. The band offsets were found strongly dependent on the strain modes and interface structures. These results suggest that in epitaxial growth of ZrO_2 on Si for gate dielectric applications, the chemical environment should be well controlled to get reproducible band offsets.

DOI: 10.1103/PhysRevB.72.045327 PACS number(s): 73.20.At, 68.35.−p

I. INTRODUCTION

With the rapid downscaling of Si-based complementary metal-oxide-semiconductor (CMOS) devices, the search for a gate dielectric to replace Si dioxide in CMOS devices has become an urgent task.[1,2] Among many possible candidates, group IV B metal oxides, HfO_2 and ZrO_2, have been studied extensively[3–7] and stand out as the leading contenders. However, the oxides of Hf and Zr with an amorphous interface layer (SiO_2 or metal silicate) will no longer be tolerable after one or two generations because the interfacial layer limits the minimum achievable *equivalent oxide thickness* (EOT) value. Epitaxial crystalline metal oxide with atomically well-defined interface with Si will be required. However, the atomic structure of metal oxide and Si interface remains to be understood, as epitaxial growth of Hf and Zr oxides on Si is still a challenge. Recently, theoretical approach based on the first-principles density functional theory (DFT) has been used to study interfacial properties of metal oxide dielectric/Si interface on atomic level.[8–14] The general bonding rules proposed by Robertson and Peacock[10] are very instructive in understanding the atomic structure of oxide/Si interfaces, and such rules have been tested for several model interfaces of ZrO_2/Si in free-standing mode,[10] in which both the oxide and Si were relaxed simultaneously in DFT calculations. Puthenkovilakam *et al.*[12] studied the detailed atomic and electronic structures of ZrO_2/Si interfaces using first-principles calculations. The valence band offset (VBO) evaluated from their interface model agrees with their x-ray photoelectron spectroscopy (XPS) experimental results (3.65 eV),[15] which indicated that the conduction band offset (CBO) is smaller than the critical value for high-*k* dielectric applications. However, there have been other reported experimental values for the valence band offsets, e.g., 3.0 eV in Ref. 7 and 3.2 eV in Ref. 16. Such variations indicate that band offsets are deposition-process dependent. Thus, further study is required in order to clarify the dependence of band offset on interface structure.

In this work, atomic structure and electronic properties of various ZrO_2/Si interface models are studied. The stabilities of these interfaces are compared to explore the possibility of atomic control of interface structure by altering the chemical environment (oxygen chemical potential). The valence band offsets for the various interface structures are calculated to determine the dependence of band offset on interface structures, thus to provide information for band offset engineering with these materials.

II. METHOD

DFT calculations were performed by using the Vienna ab-initio simulation package (VASP)[17,18] code and partially checked by Cambridge sequential total energy package (CASTEP),[19] with Vanderbilt ultrasoft pseudopotentials[20] and the generalized gradient approximation (GGA)[21] for the exchange-correlation potential. Previous *ab initio* studies of bulk zirconia[22] and surface[23] have shown that it is necessary to include generalized gradient corrections in order to accurately describe the bulk energy differences between the various polytypes of ZrO_2 and the surface energy of ZrO_2. In addition, GGA is more suitable to studies of interfaces which represent a more inhomogeneous chemical environment. A cutoff energy of 350 eV was used in the plane wave expansion of electron wavefunction. For the primitive cell of bulk tetragonal ZrO_2 (t-ZrO_2), we used an $8\times8\times6$ Monkhorst–Pack k mesh, and for the (1×2) interface supercells ($3.858\ \text{Å}\times7.716\ \text{Å}\times35.000\ \text{Å}$), an $8\times4\times1$ k mesh. Electronic optimization was performed using a fairly robust mixture of the blocked Davidson and the residual minimization method-direct inversion in the iterative subspace (RMM-DIIS) algorithm as implemented in VASP. Ionic relaxation was performed using the conjugate gradient (CG) algorithm. Density of states (DOS) were calculated with finer k meshes using the tetrahedron method with Blöchl corrections as implemented in VASP.

 ©2005 The American Physical Society

III. BULK Si AND ZIRCONIA STRUCTURES

Zirconia has three polymorphs which are, in sequence of stability from low to high temperature, monoclinic phase (m-ZrO_2), tetragonal phase (t-ZrO_2), and cubic phase (c-ZrO_2). Our calculation correctly reproduced the energetic hierarchy among the three phases. The m-ZrO_2 is favored over t-ZrO_2 by 77 meV/formula unit and over c-ZrO_2 by 156 meV/formula unit, which are in excellent agreement with other DFT calculations and the experimental results.[22] Both c-ZrO_2 and t-ZrO_2 are suitable for epitaxial growth on Si. In this study, t-ZrO_2 is used as the building block. The simple reason is that the phase transition from c-ZrO_2 to t-ZrO_2 is barrierless when both are imposed by the tetragonal symmetry. The unstrained crystalline structures are well reproduced with $a=5.456$ Å for Si and $a=3.650$ Å, $c/a=1.449$, $dz=0.0512$ for t-ZrO_2, compared to the experimental values of $a=5.45$ Å for Si and $a=3.64$ Å, $c/a=1.448$, $dz=0.065$ for t-ZrO_2.[24] These theoretical lattice constants agree well with those of other DFT calculations.[20,25] For the epitaxial growth of t-ZrO_2 on Si (001) substrate, the t-ZrO_2 is in-plane strained with $a_{\parallel}=a_{Si}/\sqrt{2}=3.858$ Å and the lattice parameter c in the interface normal contracted to 5.200 Å accordingly. A uniaxial strain along [001] will not change the symmetry of t-ZrO_2 ($P4_2/nmc$), but it leads to two dramatic changes in the band structure of t-ZrO_2, as shown in Fig. 1. One is the substantial reduction of the indirect band gap, from 4.0 to 2.9 eV. The other is the disappearance of the conduction band (CB) gap between Zr $4d$ (x^2-y^2,z^2) and Zr $4d$ (xy,$yz.xz$) states.

IV. INTERFACE STRUCTURES

For the interface structure of epitaxial t-ZrO_2 (001) on Si (001), there are many possibilities even for abrupt interfaces. We chose the interface structures based on the general bonding rules for Si and ionic oxides interfaces, recently proposed by Robertson and Peacock.[10] The general bonding rules state that: (1) terminate with faces with enough excess oxygen so that the interfacial Si DBs are formally Si^+ and empty, or (2) terminate with excess metal so that the Si DBs are formally Si^- and filled. The rules set valence requirements for Si and ionic interfaces. Such simple electron-counting arguments aim to give insulating interfaces because a perfect interface with no electronic defects and no midgap interface states is a key criterion for high-k applications. Our detailed studies on various ZrO_2/Si model interfaces offer a test for such rules. Both the unreconstructed Si surface and the 2×1 reconstructed Si surface are considered as the growth templates. The various interface structures are shown in Fig. 2. While many other interface structures, such as that with a mixed Si-Zr layer in Ref. 8, are possible, we consider only the abrupt interfaces in this study. Some of the ZrO_2 on unreconstructed Si surface structures (**a**, **b**, **d**, and **e**) are proposed by Robertson and Peacock[10] and structure **f** was proposed by Puthenkovilakam *et al.*[12] Structure **a** is an ideal Si:OOZrO interface. Two adjacent Si dangling bonds are first saturated by a bridge O. Then the closed OZrO shell is stacked above it with the interface Zr standing on the shoulder of the two bridging Os. To get structure **b** and **c**, we simply translate the OZrO stacks in the interface plane. For **b**, interface Zr stands on the head of the bridge O and for **c**, on the shoulder of two interface Si atoms. The surface Si dangling bonds can also be saturated by metal atoms, such as structures **d** and **e**. Such silicide interfaces are expected to be metallic. We also consider models formed by the t-ZrO_2 and the 2×1 reconstructed silicon surface structures. Structure f and h are such structures with the dangling bond on each Si surface atom first saturated by an O atom. Structure **g**, **i**, and **j** are three interface structures with oxidized Si dimmer. All the five structures (**f**, **g**, **h**, **i**, **j**) are O terminated (the surface Si are saturated by O). The Zr-terminated structures on the 2×1 reconstructed silicon surface are not considered because earlier DFT calculations[26] showed that the adsorbed Zr is thermodynamically unstable against the formation of bulk silicide $ZrSi_2$, which are technologically unfavorable.

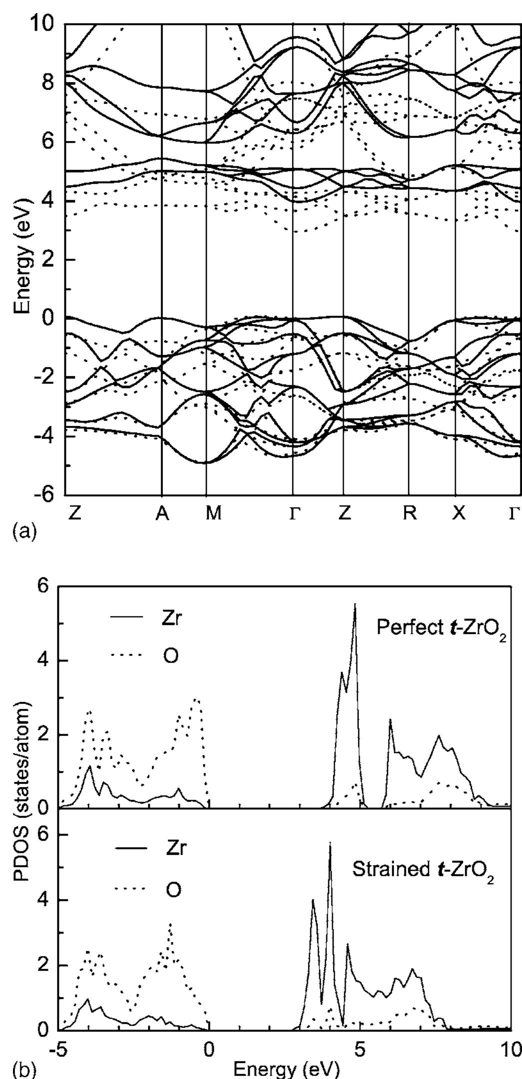

FIG. 1. Band structures (a) and PDOS (b) for perfect t-ZrO_2 and in-plane strained t-ZrO_2. Solid lines: perfect t-ZrO_2; dotted lines: in-plane strained t-ZrO_2.

The ZrO_2-Si interfaces are modeled following a supercell approach with repeated slab geometry. The slab includes eight layers of Si, five layers of t-ZrO_2, and at least 10 Å

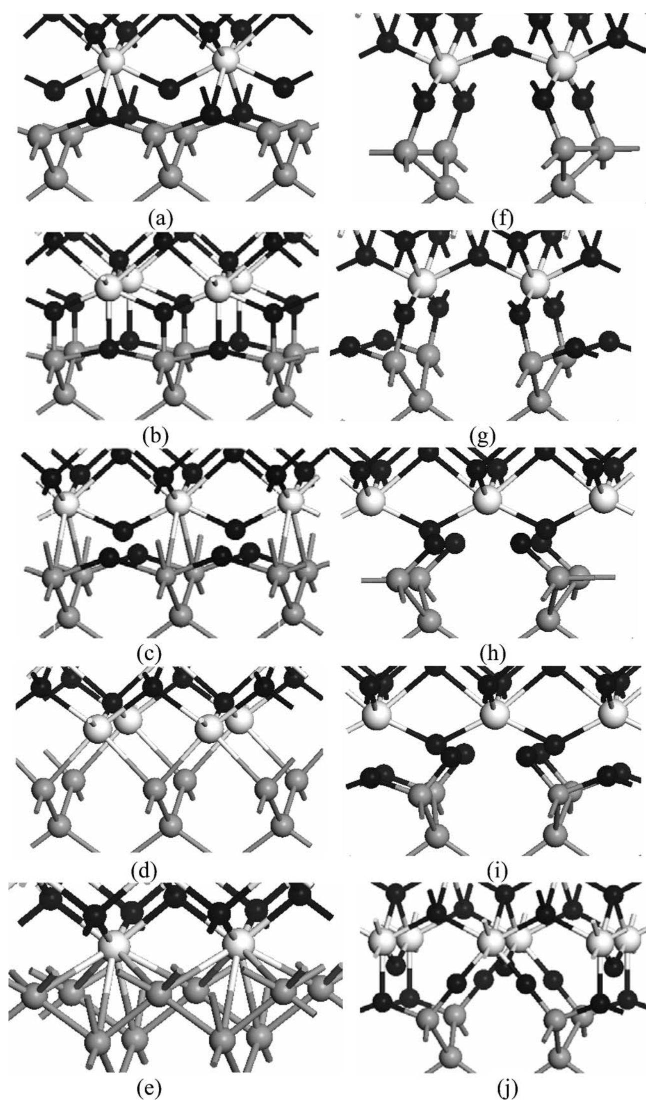

FIG. 2. Model interfaces for t-ZrO_2/Si, viewed in the (110) plane (gray: Si; black: O; light: Zr).

vacuum. The bottom Si layer is saturated with two hydrogen atoms per Si. The positions of the hydrogen atoms and the last Si layer are fixed during relaxation. All the other atoms are allowed to move to minimize the total energy without any symmetry restriction. The prestrained t-ZrO_2 ($\sqrt{2}\,a = 5.456$ Å, $c = 5.200$ Å) and unstrained Si were used as the building blocks. In this case, the relaxations occur only in the first two interface-neighboring (for t-ZrO_2 also the surface) layers.

V. ELECTRONIC STRUCTURES AT THE INTERFACE

The relaxed interface supercells were used to calculate the total DOS and the projected density of states (PDOS) on different atoms. Due to the large size of our supercells, a nonselfconsistent calculation of DOS with much denser k meshes follows a self-consistent total energy calculation with fewer k points. Figure 3 shows the total DOS and PDOS on different atoms residing in different layers for structure **a**. It is clear that the PDOS for atoms residing in the middle layers converge to their respective bulk characters. From the site-projected DOS for the interface Si and Zr atoms for structure **a** shown in Fig. 3, the absence of the interface induced mid-gap state demonstrates semiconductor character of the interface structure. Similar total DOS and PDOS have also been obtained for structures **b**, **g**, **h**, **i**, and **j**, which all show semiconductor character. For structure **c**, because of the adjacent Zr and Si atoms, there are interface states in the middle of Si band gap (not shown here). Subsequent energetic calculations show that this structure is unstable, and we will not discuss it in detail. Structures **d** and **e** have silicidelike bonds, and should be metallic although they satisfy the general bonding rules. This was confirmed by the calculated DOS and PDOS shown in Fig. 4. There is no band gap for these two structures. For both structures, the PDOS for the interface Zr atoms are metal-like. For **d**, the tetrahedral bonds are satisfied for interface Si atoms, so the interfacial Si DBs are nearly occupied, while for **e**, the interfacial Si DBs are partially occupied. Our result for structure **d** is different from that of Robertson and Peacock,[10] where an insulating interface with states in the middle gap has been found for structure **d**. Such a difference may come from the different Zr-Si bond length and angles in the interface when the interface supercell relaxed using different strain modes. Our results indicate that the general bonding rules are not applicable for silicidelike Zr-Si interface bonds. That means termination of Si DBs with excess Zr cannot give an insulating interface. The entire family of O-terminated interface structures, both on unreconstructed Si and 2×1 reconstructed Si templates, satisfy the bonding rules, and yield insulating interfaces. This is not surprising since the general bonding rules, or electron counting arguments, are based on valence requirements, and the metal bonds in the interface do not obey such rules.

The PDOS of the O and Si atoms residing in the middle layer of the respective material (referred to as bulk-O and bulk-Si, respectively) in various structures are shown in Fig. 5. The valence band maxima (VBM) of Si PDOS have been aligned at energy zero. We can see a rigid shift of the relative energy position of O and Si, as shown in Fig. 5. This shift is due to the change of the net interface dipole. In fact, such PDOS has been used to calculate the valence band offsets (VBOs) directly, a direct density of states analysis technique.[9] Because of the semiquantitative character of PDOS (nonperfect determination of the VBM from PDOS), we prefer the standard "bulk-plus-lineup"[27,28] procedures of calculating VBO. Nevertheless, such a rigid shift in PDOS indicates variation of valence band offsets between different interface structures.

VI. INTERFACE ENERGETICS

The relative stability of an interface is given by its formation energy. The smaller the interface formation energy, the more stable the interface structure. For the repeated slab structure, the interface formation energy can be expressed as

$$E_{form} = \frac{E_{total} - [nE_{ZrO_2} + mE_{Si} + E_{other} \pm l\mu_O]}{A}, \qquad (1)$$

where E_{total} is the DFT total energy of the interface supercell, n and m are the numbers of Si and ZrO_2 bulk units, respec-

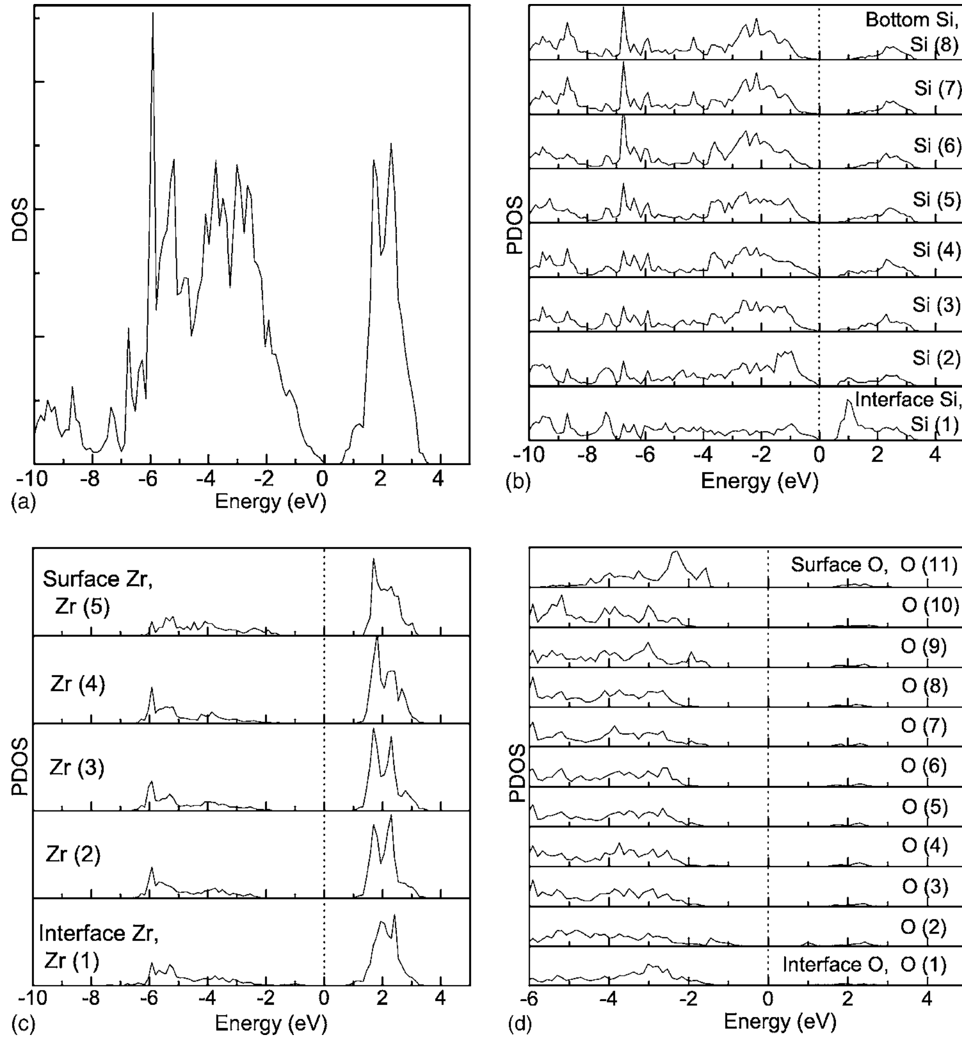

FIG. 3. Total DOS (a) and PDOS of Si (b), Zr (c), and O (d) for structure **a**. The energy of the valance band maximum is set to zero.

tively, E_{Si} and E_{ZrO_2} are the total energy per Si and ZrO_2 bulk unit, respectively, E_{other} includes the upper surface energy of ZrO_2 and the energy related to the H atoms, l is the number of oxygen atoms added (+, for O-rich situation) or removed (−, for Zr-rich) to create the interface, μ_O is the chemical potential of oxygen in the interface supercell, and A is the basal area of the interface supercell. E_{ZrO_2} corresponds to the in-plane strained t-ZrO_2 bulk (in the same strain state as in the slab), so the calculated interface formation energy is volume independent.[29] We used the DFT total energies instead of the Gibbs free energies, since the vibrational entropy contributions and enthalpy changes due to finite temperature are almost the same for different structures and will not change the relative stability of different structures significantly. For the various repeat slab interface supercell structures being considered, $[nE_{ZrO_2}+mE_{Si}+E_{other}]$ is the same and can also be counteracted when the relative interface energies are compared. The key problem is to evaluate the chemical potential of the added or subtracted O atoms. Here we utilized the method which has been widely used to calculate the surface energy of metal oxide.[30–32] We assumed that Zr bulk and O_2 gas reservoirs are in thermal equilibrium with the ZrO_2 thin film (if this is not the case, the ZrO_2 thin film would either grow or decompose). This requires

$$2\mu_O + \mu_{Zr} = E_{ZrO_2}, \tag{2}$$

where E_x and μ_x are the DFT total energies and chemical potentials of particle x, respectively. By defining the formation enthalpy (by convention is negative) as

$$H_f = E_{ZrO_2} - (E_{O_2} + E_{Zr}), \tag{3}$$

where E_{O_2} and E_{Zr} are the DFT total energies per oxygen molecule and Zr atom in hcp-Zr bulk, respectively, we get

$$(2\mu_O - E_{O_2}) + (\mu_{Zr} - E_{Zr}) = H_f. \tag{4}$$

Because of the simple fact that the chemical potential for each element cannot be above that of the bulk (or gas) element phase,[33] μ_O is allowed to vary over the range

$$\tfrac{1}{2}(E_{O_2} + H_f) \leqslant \mu_O \leqslant \tfrac{1}{2}E_{O_2}. \tag{5}$$

Once the bound for the chemical potential of oxygen has been found, the interface formation energy can be expressed as a function of μ_O, as in Eq. (1). In the following calcula-

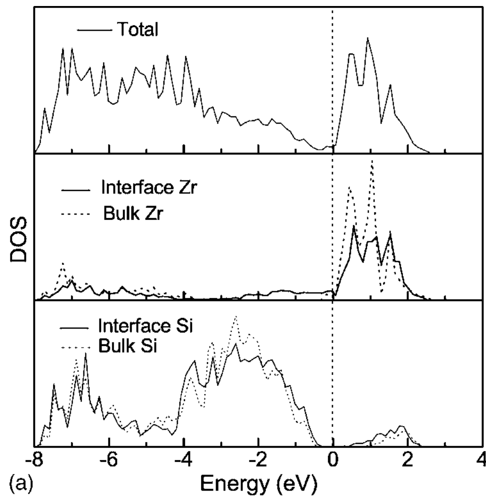

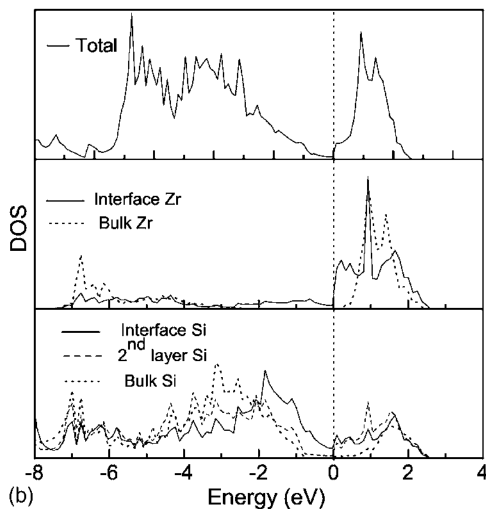

FIG. 4. Total DOS and PDOS for structure **d** (a) and **e** (b). The zero energy is at the Fermi level.

tion, all energies and chemical potentials are referenced to $\frac{1}{2}E_{O_2}$.

Following the approach outlined above, we first calculated the relative interface formation energies for the ten interface structures as a function of oxygen chemical potential, with respect to the stoichiometric structure **f**. Then the absolute formation energy of structure **f** was determined to be 0.079 eV/Å,[2] using the supercell structure without vacuum. Finally, the absolute formation energies of the various structures as a function of μ_O are shown in Fig. 6. The dashed lines are for unreconstructed Si surface template, while the solid lines for the 2×1 reconstructed Si surface template. The left and right boundaries of Fig. 6 correspond to the limiting cases of metallic zirconium and molecular oxygen, respectively. The most important features of Fig. 6 are: (i) Among all the interface structures, structure **b** seems to be the most stable one except in the very low O chemical potential region. So this structure is most possible for our high-resolution transmission electron microscopy (HRTEM) image;[4] (ii) the Zr-terminated interface structures only exist in very low oxygen partial pressure; (iii) for the reconstructed template, the most stable structure is O chemical

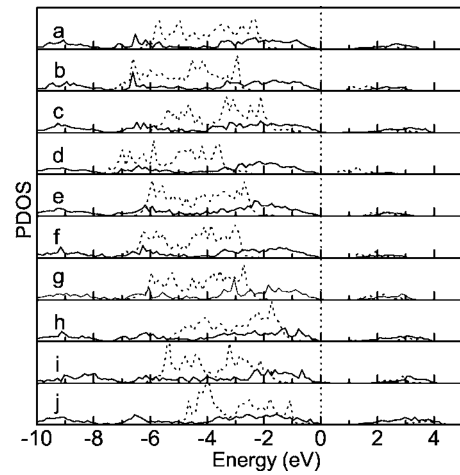

FIG. 5. PDOS of bulk-Si and bulk-O atoms for the various structures (solid lines: Si; dotted lines: O). The zero energies are aligned at the Si VBMs.

potential dependent, with the increase of μ_O, the most stable structure is structure **f**, **g**, and **j** by sequence; and (iv) the Si-dimer position are easier to be attacked by O for structure **f** compared to **h**. Structure **g**, the Si-dimer-oxidized variant of structure **f**, is more stable than **f** in most region of μ_O; while structure **h** and its Si-dimer-oxidized variant **i** have almost the same average formation energy in the allowed O chemical potential region. The formation energies of the various interfaces at their respective most favored growth conditions (the limiting cases of metallic zirconium for metal-rich interfaces and molecular oxygen for oxygen-rich interfaces) are also shown in Table III, which are comparable to the results obtained by Fiorentini and Gulleri[8] using the Si-epi structure ZrO_2 bulk to build the interfaces.

From the above analysis, we can determine the equilibrium composition and geometry of an interface structure in contact with a given chemical environment (O chemical potential) from the thermodynamics point of view, which provides the possibility of the atomic-scale control of the inter-

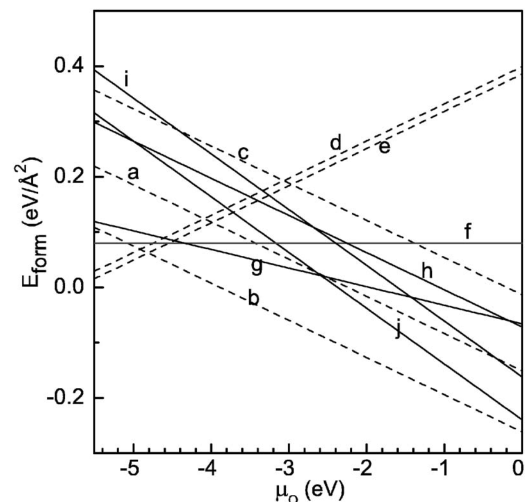

FIG. 6. Interface formation energies (E_{form}) of the various structures as a function of oxygen chemical potential (μ_O).

face structure by altering the chemical environment. However, we should caution that the above discussion is based only on thermodynamic arguments. The real situation in epitaxial thin film growth is more complicated where kinetic effects also play an important role. Nevertheless our calculated interface formation energy dependence on O chemical potential does offer the possibility of the atomic-scale control of the interface structure.

VII. BAND OFFSETS

For high-k applications, the conduction band offset between the high-k dielectric material and Si should be large enough (>1.0 eV) to give an accessible low leakage current. Given the experimental band gap difference ΔE_g for dielectric material and Si, the relation between CBO and VBO can be expressed by

$$\mathrm{CBO} + \mathrm{VBO} = \Delta E_g. \tag{6}$$

Because of the band gap error in GGA, we will focus on the DFT calculation of VBO and the CBO then can be found using formula (6) with ΔE_g of 4.7 eV (1.1 eV for Si and 5.8 eV for ZrO_2). Based on our calculation, in-plane tensile strain has the tendency to decrease the band gap value of t-ZrO_2. However, there are no experimental results for the band gap of strained t-ZrO_2.

The interface valence band offsets are evaluated by using the standard bulk-plus-lineup[27,28] procedure, where the VBO is usually split into two terms

$$\mathrm{VBO} = \Delta E_V + \Delta V. \tag{7}$$

The first term is referred as the band structure term. It is defined as the energy difference of the valence band edges as obtained from two independent bulk calculations. The quasiparticle corrections to the bulk valence-band edges at the GW level are essential because the corrections are substantial for oxides and cannot counteract between Si and oxides.[34–36] Same as in Ref. 8, we apply an overall correction of 1.08 eV to all the Si-ZrO_2 interface structures, with 0.15 eV for Si[33] and 1.23 eV for ZrO_2.[35] This correction to the DFT-GGA band offset is necessary in order to compare the calculated values with experimental results. The second term in Eq. (7) is the lineup of the average of the electrostatic potential through the interface, which can be obtained using the double-macroscopic average technique.[28,37] As such macroscopic quantity summarizes all the intrinsic interface effects,[37,38] the change of the chemical composition in the interface (interface structures) can modify this term; we will discuss this in detail in Sec. VII B. The only assumption used in this bulk-plus-lineup procedure is that for one specified constituent such as Si or ZrO_2, the energy difference between the VBM and macroscopic electrostatic potential is kept constant in bulk and interface. This assumption has been validated by XPS measurement for $SrTiO_3$ on Si heterostructure,[39] where the core levels (which are very like electrostatic potential here in spirit[38]) are used to lineup the band structures. The band bending at the interface is negligible, because its length scale, of the order of Debye length, can be as long as several thousands angstroms in low doped semiconductor.[38]

TABLE I. Values of parallel, perpendicular lattice parameters and E_V for Si and t-ZrO_2 under different strain conditions. (For an easier comparison, Si lattice parameters are given in the notation of t-ZrO_2 structure.)

System	$a_\parallel$ (Å)	$a_\perp$ (Å)	E_V (eV)
Si	3.858	5.456	4.83
	3.659	5.656	5.75
	3.674	5.640	5.67
t-ZrO_2	3.650	5.289	1.70
	3.858	5.200	1.58
	3.659	5.284	1.69
	3.674	5.276	1.66

In band-offset engineering (modifying the band discontinuity at semiconductor heterojunctions), the structural (i.e., of uniaxial deformation and/or lattice distortions.) and chemical effects (i.e., of different interface chemical compositions) have been studied for isovalent and heterovalent lattice-mismatched interfaces.[26,35] As for the structural effects few works have been done for the crystalline metal oxide on Si structures, while lattice mismatch is the case for most crystalline metal oxide on Si structures. The lattice mismatch between t-ZrO_2 and Si is as high as 6%. As for the chemical effects, the band offsets can be engineered by controlling the interface chemical structures, as proved recently in epitaxial-$SrTiO_3$/Si interfaces.[11] But for the epitaxial-ZrO_2/Si interfaces, detailed study is needed.

A. Strain mode effects on band offsets

To study the structural effects on band offsets, we used two modes, free-standing mode and Si-substrate mode, to relax the interface supercell structures. Here we used 1×1 supercell geometry, with nine layers of Si, five layers of t-ZrO_2, and no vacuum. In the free-standing mode calculation, all the three lattice parameters and atom positions are allowed to relax to minimize the DFT total energy. In this way, both ZrO_2 and Si are strained with ZrO_2 being compressed and Si elongated in the direction perpendicular to the interface. This is similar to the structure of a superlattice consisting of alternating thin Si and ZrO_2 layers. For the Si-substrate mode, the lateral lattice parameter is set to the theoretical value of bulk Si ($a_{\mathrm{Si}}/\sqrt{2}=3.858$ Å). The prestrained t-ZrO_2 was used as the building block. Internal coordinations and vertical cell size are optimized to get the ground state. This mimics the situation of epitaxial growth of ZrO_2 thin film on thick Si substrate, where the strain only resides in ZrO_2 thin film. To demonstrate the strain mode effects on band offsets, structure **a** and **e** are relaxed in two modes separately.

Table I shows the values of E_V, the energies for the highest occupied VBM states measured relative to the respective average of electrostatic potential, for ZrO_2 and Si bulk under different strain conditions. We note that the uniaxial strain

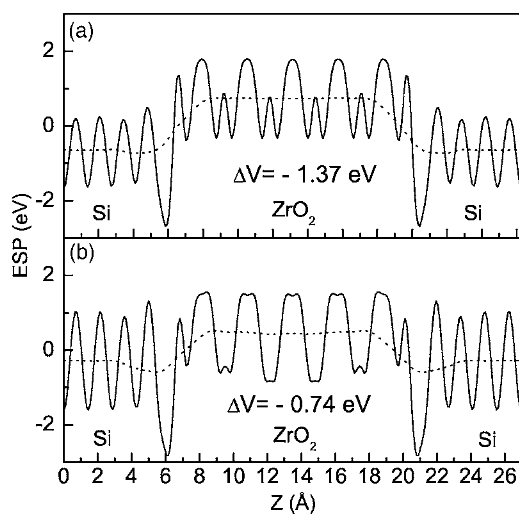

FIG. 7. Planar (solid line) and macroscopic average (dotted line) of ESP for structure **a** in Si-substrate mode (a) and free-standing mode (b), respectively. ΔV is the lineup.

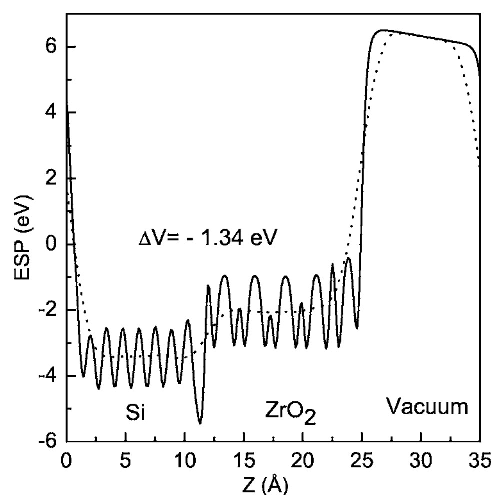

FIG. 8. Planar (solid line) and macroscopic average (dotted line) of ESP for structure **a** in repeated slab supercell. ΔV stands for the lineup.

along [001] raises the value of E_V of Si dramatically ($\sim$0.9 eV) but the in-plane tensile strain only changes the value of E_V of t-ZrO_2 slightly ($\sim$0.1 eV), which reflects the insensitivity of the highest occupied molecular orbital (HOMO) nonbonded oxygen p states. Since the VBO components from the ZrO_2 bulk change little with the strain states of ZrO_2, it is likely that a loss of pseudomorphicity of the oxide film does not change too much the VBO, whereas the strain state in the Si side contributes to most of the changes in VBO. Figure 7 shows the planar and double macroscopic average of the electrostatic potential (ESP) for structure **a** in free-standing mode, and Si-substrate mode, respectively. The lineup ΔV is the difference between the double macroscopic averaged potentials residing in Si and ZrO_2 bulklike regions, respectively. The values of ΔE_V, ΔV, and VBO (with and without GW correction) are summarized in Table II for structures **a** and **e** under the two strain modes. The main conclusions that can be drawn from Table II are: (i) the band structure term ΔE_V has a noticeable variation under different strain modes, which is mainly due to the dramatic raise of E_V of strained Si; (ii) the strain mode effect on potential lineup is interface-structure dependent which is supposed to be related to the change of net dipole at the interface; (iii) for a given interface structure, the variation of the VBO with the strain modes are substantial; and (iv) with GW corrections, the VBOs from Si-substrate mode is closer to the experimental value (3.0–3.6 eV), which is reasonable because Si-substrate mode is the situation for experimental thin film growth.[7,15,16] By comparison, our VBOs without GW corrections for the free-standing mode are slightly higher than but close to the values reported by Robertson and Peacock,[10] who used a direct PDOS analysis technique. From the above analysis, we can see that it is not appropriate to compare the band offsets obtained from the free standing mode with the experiment results as the x-ray photoelectron measurements for valence band offsets were made on high-k dielectric thin films grown on unstrained Si substrate. In Sec. VII B, band offsets for various interface structures in Si-substrate mode were calculated and compared to the experimental values.

TABLE II. VBO for structure **a** and **e** in two strain modes: Si-substrate (SS) and free-standing (FS) modes.

Structure	**a**-SS	**e**-SS	**a**-FS	**e**-FS
$a_\parallel$ (Å)	3.858	3.858	3.659	3.674
ΔE_V (eV)	3.25	3.25	4.06	4.01
ΔV (eV)	−1.37	−0.93	−0.74	−0.92
VBO (eV)	1.88	2.32	3.32	3.05
+GW (eV)	2.96	3.40	4.40	4.13

B. Interface structure effects on band offsets

As mentioned earlier, the interface structure or interface chemical composition can modify the lineup of VBO, which has been demonstrated in many semiconductor heterostructures.[28] To obtain the potential lineup for the different interface morphologies described in Sec. II, we performed calculations using the repeated slab supercell. All supercell structures are relaxed in Si-substrate mode mentioned above. The planar average and double macroscopic average of the ESP for structure **a** with repeated slab supercell is as shown in Fig. 8. The calculated values of ΔV are summarized in Table III for all the ten interface structures. From the virtual gap state (VGS) model (in this model, the VBO is interface structure independent), Robertson[40] obtained the VBO for ZrO_2/Si heterostructures of 3.1 eV. Such VGS value plus the contribution from the interface net dipole gives the VBO in real situation. Our calculated VBOs is higher (lower) than such VGS value (3.1 eV) as the positive (negative) interface dipole effects have been included automatically in the bulk-plus-lineup procedure. Puthenkovilakam *et al.*[12] obtained the VBO of 3.89 eV for structure **f**, in reasonable agreement with our result of 3.74 eV.

TABLE III. Interface formation energies (E_{form}) and VBO for the various structures. E_{form} are for the structures at their respective most favored growth conditions (the limiting cases of metallic zirconium for metal-rich interfaces and molecular oxygen for oxygen-rich interfaces). The relative stable structures are highlighted with bold characters. All GW corrections are included for the VBO.

Structure	E_V (eV)	ΔV (eV)	VBO (eV)	E_{form} (eV/Å^2)
a	3.25	−1.34	**2.99**	**−0.15**
b	3.25	−0.29	**4.04**	**−0.26**
c	3.25	−1.79	2.54	−0.01
d	3.25	−0.31	4.02	0.03
e	3.25	−1.01	3.32	0.02
f	3.25	−0.59	3.74	0.08
g	3.25	−0.92	**3.41**	−0.06
h	3.25	**−2.48**	**1.85**	**−0.07**
i	3.25	−1.80	**2.53**	**−0.16**
j	3.25	−2.80	**1.53**	**−0.24**

It is clear from Table III that the valence band offset is strongly dependent on the interface structure or the interface chemical composition strongly modifies the lineup term of VBO, as the case in CaF_2/Si heterostructures.[41] The variation of the band offset between different structures is supposedly due to the change of interface net dipole. As shown in Fig. 5, the change of the interface dipole forces a rigid shift of the energy position of the materials on both sides of the interface. In Table III, the relative stable structures have been highlighted with bold characters. Even for these structures, the difference is as large as 2.5 eV. Such large variations with interface structures bring some technological difficulties, that is, the chemical environment should be well controlled to achieve reproducible band offset. Such a conclusion drawn from the model interfaces relaxed in the Si-substrate mode is different from that in the free-standing mode, where a relatively constant band offset has been found for O-terminated models.[10] As we have shown, such differences can be due to two effects: the structural (uniaxial deformation) and chemical (interface chemical composition) effects. The former affects both the bulk and lineup terms of band offsets, while the latter only affects the lineup term. Our results can offer some explanation for the different experimental results which vary from 3.0 to 3.6 eV. This difference may be due to different interface structures. However, it is difficult to make quantitative comparison directly because the samples used in the experiments[7,15,16] are inhomogeneous and far from perfect epitaxial crystal ZrO_2 on Si structure.

VIII. SUMMARY

The atomic and electronic structures of various ZrO_2/Si model interfaces have been studied using first-principles DFT calculations. The general bonding rules have been tested for our structures in Si-substrate mode, and it was found that such rules are not followed by metal-terminated interfaces where the silicidelike bonds give a metallic interface, which was not always the case in free-standing mode.[10] The interface energetics analysis was carried out to compare the relative stability of interface structures. The result shows that the stable interface structure is oxygen chemical potential dependent, which provides the possibility of atomic-level control on interface structure by altering the chemical environment. The calculated band offset reveals crucial sensitivity to the interface structures. The chemical environment should be well controlled to achieve desired band offset.

*Author to whom correspondence should be addressed. Email address: phyfyp@nus.edu.sg

[1] A. I. Kingon and S. K. Streiffer, Nature (London) **406**, 1032 (2000).

[2] G. D. Wilk, R. M. Wallace, and J. M. Anthony, J. Appl. Phys. **89**, 5243 (2001).

[3] M. Copel, M. A. Gribelyuk, and E. Gusev, Appl. Phys. Lett. **76**, 436 (2000).

[4] S. J. Wang, C. K. Ong, S. Y. Xu, P. Chen, W. C. Tjiu, J. W. Chai, A. C. H. Huan, W. J. Yoo, J. S. Lim, W. Feng, and W. K. Choi, Appl. Phys. Lett. **78**, 1604 (2002).

[5] S. J. Wang and C. K. Wong, Appl. Phys. Lett. **80**, 2541 (2002).

[6] J. P. Chang and Y. S. Lin, Appl. Phys. Lett. **79**, 3666 (2001).

[7] C. C. Fulton, G. Lucovsky, and R. J. Nemanich, Appl. Phys. Lett. **84**, 580 (2004).

[8] V. Fiorentini and G. Gulleri, Phys. Rev. Lett. **89**, 266101 (2002).

[9] X. Zhang, A. A. Demkov, Hao Li, X. Hu, Yi Wei, and J. Kulik, Phys. Rev. B **68**, 125323 (2003).

[10] P. W. Peacock and J. Robertson, Phys. Rev. Lett. **92**, 057601 (2004).

[11] C. J. Forst, C. R. Ashman, K. Schwarz, and P. E. Blochl, Nature (London) **427**, 53 (2004).

[12] R. Puthenkovilakam, E. A. Carter, and J. P. Chang, Phys. Rev. B **69**, 155329 (2004).

[13] A. Fissel, J. Dabrowski, and H. J. Osten, J. Appl. Phys. **91**, 8986 (2002).
[14] P. W. Peacock and J. Robertson, Appl. Phys. Lett. **83**, 5497 (2003).
[15] R. Puthenkovilakam and J. P. Chang, Appl. Phys. Lett. **84**, 1353 (2004).
[16] S. Miyazaki, J. Vac. Sci. Technol. B **19**, 2212 (2001).
[17] G. Kresse and J. Hafner, Phys. Rev. B **47**, R558 (1993); **48**, 13115 (1993).
[18] G. Kresse and J. Furthmuller, Comput. Mater. Sci. **6**, 15 (1996); G. Kresse and J. Furthmuller, Phys. Rev. B **54**, 11169 (1996).
[19] M. D. Segall, P. L. D. Lindan, M. J. Probert, C. J. Pickard, P. J. Hasnip, S. J. Clark, and M. C. Payne, J. Phys.: Condens. Matter **14**, 2717 (2002).
[20] D. Vanderbilt, Phys. Rev. B **41**, R7892 (1990).
[21] J. P. Perdew, J. A. Chevary, S. H. Vosko, K. A. Jackson, M. R. Pederson, D. J. Singh, and C. Fiolhais, Phys. Rev. B **46**, 6671 (1992).
[22] G. Jomard, T. Petit, A. Pasturel, L. Magaud, G. Kresse, and J. Hafner, Phys. Rev. B **59**, 4044 (1999).
[23] A. Christensen and E. A. Carter, Phys. Rev. B **58**, 8050 (1998); **62**, 16968 (2000).
[24] C. J. Howard, R. J. Hill, and B. E. Reichert, Acta Crystallogr., Sect. B: Struct. Sci. **44**, 116 (1988).
[25] A. Eichler, Phys. Rev. B **68**, 205408 (2003).
[26] C. J. Forst, P. E. Blochl, and K. Schwarz, Comput. Mater. Sci. **27**, 70 (2003).
[27] C. G. Van de Walle and R. M. Martin, Phys. Rev. B **34**, 5621 (1986).
[28] A. Baldereschi, S. Baroni, and R. Resta, Phys. Rev. Lett. **61**, 734 (1988); M. Peressi, N. Binggeli, and A. Baldereschi, J. Phys. D **31**, 1273 (1998).
[29] F. Bernaldini and V. Fiorentini, Phys. Rev. B **57**, R9427 (1998).
[30] J. Padilla and D. Vanderbilt, Surf. Sci. **418**, 64 (1998).
[31] K. Reuter and M. Scheffler, Phys. Rev. B **65**, 035406 (2002).
[32] A. Eichler and G. Kresse, Phys. Rev. B **69**, 045402 (2004).
[33] G. X. Qian, R. M. Martin, and D. J. Chadi, Phys. Rev. B **38**, 7649 (1988).
[34] X. Zhu and S. G. Louie, Phys. Rev. B **43**, 14142 (1991).
[35] B. Kralik, E. K. Chang, and S. G. Louie, Phys. Rev. B **57**, 7027 (1998).
[36] J. Junquera, M. Zimmer, P. Ordejon, and P. Ghosez, Phys. Rev. B **67**, 155327 (2003).
[37] L. Colombo, R. Resta, and S. Baroni, Phys. Rev. B **44**, 5572 (1991).
[38] A. Franciosi and C. van de Walle, Surf. Sci. Rep. **25**, 1 (1996).
[39] S. Chambers, Y. Liang, Z. Yu, R. Droopad, J. Ramdani, and K. Eisenbeiser, Appl. Phys. Lett. **77**, 1662 (2000).
[40] J. Robertson, J. Vac. Sci. Technol. B **18**, 1785 (2000).
[41] S. Satpathy and R. M. Martin, Phys. Rev. B **39**, 8494 (1989).